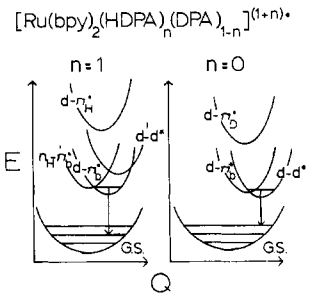

Figure 11. Potential energy diagrams of the ground and excited states for the complexes $[Ru(bpy)_2(HDPA)_n(DPA^-)_{1-n}]^{(1+n)+}$ (n = 1, 0). Energy is plotted vs. a vibrational mode Q, such as the totally symmetric Ru–N stretch. The orbital origin of the excited states are as indicated. No implication of the relative force constants is intended (GS, ground state; H, HDPA; D, DPA^-; b, bpy).

$(DPA^-)_3]^-$ would be due to the disappearance of the ILCT $n_{HDPA^-}\pi_{DPA^-}{}^*$ state since the lone-pair nitrogen electrons of the DPA^- ligand are involved with "l-type"[43] conjugation and thus no low-energy n–π^* state can exist.

However, turning off the n–π^* ILCT emission in the mixed-ligand bpy(DPA^-) complexes still does not explain the disappearance of emission from the Ru–bpy chromophore. Deprotonation of the HDPA ligand, forming the more planar DPA^- ligand that does not have complete conjugation (l-type instead of "true" π conjugation), would further destabilize the metal-to-ligand σ bonds and, as previously mentioned, lower the energy of the d–d* state (Figure 11). In addition geometric distortions have been suggested for the $[Ru(bpy)_n(DPA^-)_{3-n}]^{(n-1)+}$ (n = 1, 2) complexes[26] which again imply perturbations at the metal resulting in a lowering in energy of the d–d* states. This red-shifted, weak d–d* emission was not observed for any of these complexes.

Since the deprotonation of these complexes is totally reversible, photochemical deactivation pathways do not appear to be activated and are not likely the origin of the disappearance of the luminescence.

Conclusion

The identification of a dual emission for a Ru(II) complex as for all dual emissions has fundamental significance since the implication of the result is that independent deactivation pathways exist within the same molecule. Here the two types of emission, although "spatially isolated", are perhaps best categorized as "distinct orbital type" since the orbital origin of the two emitting excited states is different. The ILCT character of a the $n_{HDPA^-}\pi_{bpy}{}^*$ emission is unique and does point up the donor (D)–acceptor (A) character of the optical process for this system. Mixed-ligand complexes as this may afford some practical photoredox possibilities since the optical properties of this system permit selective excitation of either the $n_{HDPA^-}\pi_{bpy}{}^*$ chromophore or the $d\text{–}\pi_{bpy}{}^*$ chromophore. This ability to selectively excite one or the other emitting state is not a common feature among the dual emitting transition-metal complexes.

Acknowledgment. We are grateful to Mr. Michael Myrick for synthesizing the $[Ru(bpy)(py)_4]^{2+}$ complex and for obtaining the spectroscopic data for this complex. Gratitude is also extended to Dr. Yasuhiko Ohsawa for the original synthesis of the bpy/HDPA complexes and to Dr. David Morris and Dr. Donald Segers for earlier work on bpy/HDPA and related complexes. This work was supported by a grant the Army Research Office, Grant No. DAAL-03-86-K-0040.

(43) Kasha, M.; Rawls, H. R. *Photochem. Photobiol.* **1968**, *7*, 561.

Photochemistry of Multiply Bonded Dimolybdenum Phosphate Complexes in Acidic Solution: Photoinduced Two-Electron Oxidation of $Mo_2(HPO_4)_4^{4-}$ Ion

I-Jy Chang and Daniel G. Nocera*

Contribution from the Department of Chemistry, Michigan State University, East Lansing, Michigan 48824. *Received December 15, 1986*

Abstract: The multiply bonded dimolybdenum phosphate dimers $Mo_2(HPO_4)_4^{4-}$ and $Mo_2(HPO_4)_4^{3-}$ have been prepared and spectroscopically and electrochemically characterized. The electronic absorption spectrum of the quadruply bonded complex $Mo_2(HPO_4)_4^{4-}$ in H_3PO_4 is typical of many $M\overset{n}{-}M$ species with the $\delta^2 \rightarrow \delta\delta^*$ ($^1A_{2u} \leftarrow {}^1A_{1g}$) transition occurring at 516 nm. Cyclic voltammograms of phosphoric acid solutions of $Mo_2(HPO_4)_4^{4-}$ are characterized by two reversible waves at −0.67 and −0.25 V vs. SCE that we have attributed to the $Mo_2(HPO_4)_4^{3-/4-}$ and $Mo_2(HPO_4)_4^{2-/3-}$ couples, respectively. Oxidation of $Mo_2(HPO_4)_4^{4-}$ produces the mixed-valence dimer $Mo_2(HPO_4)_4^{3-}$, which exhibits an intense near-infrared absorption band that we have assigned to the $\delta \rightarrow \delta^*$ ($^2B_{1u} \leftarrow {}^2B_{2g}$) transition. Solid $K_3Mo_2(HPO_4)_4$ is paramagnetic and follows Curie law behavior (μ = 1.58 μ_B). The EPR spectrum of $K_3Mo_2(HPO_4)_4$ at 5 K shows an axial signal ($g_\perp$ = 1.894, $g_\parallel$ = 1.886). Whereas $Mo_2(HPO_4)_4^{4-}$ thermally reacts in 2 M H_3PO_4 to produce $Mo_2(HPO_4)_4^{3-}$ and hydrogen over a period of days, irradiation ($\lambda \geq 335$ nm) of phosphoric acid solutions of the dimer leads to the facile production of $Mo_2(HPO_4)_4^{2-}$ and hydrogen. The thermal reaction presumably results from the slow conversion of $Mo_2(HPO_4)_4^{4-}$ to yield hydrogen and $Mo_2(HPO_4)_4^{2-}$ which reacts in an ensuing comproportionation reaction with $Mo_2(HPO_4)_4^{4-}$ to produce $Mo_2(HPO_4)_4^{3-}$. In contrast, the photochemical reaction mechanism is consistent with sequential oxidation of the Mo_2 core [i.e., $Mo_2(II,II) \rightarrow Mo_2(II,III) \rightarrow Mo_2(III,III)$]. Electronic absorption spectra of the $Mo_2(HPO_4)_4^{n-}$ (n = 2–4) dimers in the ultraviolet spectral region, wavelength-dependent quantum yield measurements, and photochemical studies of Mo_2 phosphate dimers under N_2O atmospheres have led us to postulate a $\pi \rightarrow \pi^*$ ($^1A_{2u} \leftarrow {}^1A_{1g}$) parentage for the photoactive state of Mo_2 phosphato complexes. We propose that excitation of this transition leads to the direct production of hydrogen atoms which undergo subsequent reaction to produce hydrogen.

There has been a longstanding interest in the oxidation–reduction chemistry of transition-metal complexes in electronic excited states and in their application as catalysts for oxidation–reduction reactions. Although numerous studies have demonstrated the propensity of electronically excited metal complexes to exchange one electron,[1-3] many desirable redox reactions such

0002-7863/87/1509-4901$01.50/0

as small molecule activation processes involve the transfer of two or more electrons to a substrate molecule. A promising approach to multielectron reactivity along thermal reaction pathways relies on coupling formal oxidation state changes of metal centers in a polynuclear core to drive an overall multielectron transformation.[4-7] Photochemical schemes employing a similar strategy, however, have been confined to relatively few transition-metal complexes[8-12] and, to date, the systematic development of multielectron photochemistry has not yet been achieved.

A goal of our research effort is to provide general guidelines for multielectron photoreaction pathways beginning with multiply bonded metal–metal ($M^{n}M$) complexes. These dimers possess several attractive properties for their application as multielectron photoreagents. First, the electronic structure of $M^{n}M$ dimers, particularly quadruply bonded species, is well-defined,[13,14] and the lowest energy excited states of many $M^{n}M$ species are sufficiently long-lived[15] to permit their subsequent chemical reaction.[16] Second, the binuclear metal core is an electron source or sink in oxidation–reduction processes. Addition of electrons to or removal of electrons from the metal–metal bond is accompanied by facile interconversion between $M^{n}M$ dimers of different bond orders.[17-19] Finally, substrates readily add to the coordinatively unsaturated metal–metal core.[20] The ability to coordinate substrate molecules to an electronically excited, redox-active binuclear metal center has important implications in the ultimate application of $M^{n}M$ dimers as multielectron photocatalysts.

Conversion of a $M^{n}M$ dimer with a metal–metal bond order of 4 to a species of bond order 3 constitutes a two-electron process and conceptually represents the simplest multielectron transformation available to a $M^{n}M$ system. Nevertheless, previous studies of $M^{n}M$ dimers indicate two-electron processes to be exceptional reaction pathways and the excited-state reaction chemistry of $M^{n}M$ dimers has been limited primarily to single-electron photoreactions. For instance, the photochemistry of $Mo_2(SO_4)_4^{4-}$ is exemplary of typical $M^{4}M$ species: under relatively strong oxidizing conditions ($\lambda \leq 254$ nm), irradiation of $Mo_2(SO_4)_4^{4-}$ in H_2SO_4 is confined to the production of the one-electron product $Mo_2(SO_4)_4^{3-}$.[21] Presumably, the chemical instability of the triple-bond sulfate dimer precludes multielectron photochemistry. In this context, the discovery of the triple-bond phosphato complex $Mo_2(HPO_4)_4^{2-}$[22] stimulated our interest because the Mo_2 phosphate system could possibly provide insight into the mechanism of multielectron photoredox transformations of $M^{n}M$ dimers in acidic solution with the successful preparation of the quadruple-bond Mo_2 phosphate dimer. Reported herein is the synthesis and spectroscopic and electrochemical characterization of $Mo_2(HPO_4)_4^{3-}$ and $Mo_2(HPO_4)_4^{4-}$ dimers, which is conjunction with $Mo_2(HPO_4)_4^{2-}$ constitute the first homologous $M^{n}M$ series possessing bond orders of 4, 3.5, and 3 resulting from $\sigma^2\pi^4\delta^2$, $\sigma^2\pi^4\delta^1$, and $\sigma^2\pi^4$ electron configurations, respectively. We also report the two-electron photoinduced oxidation of $Mo_2(HPO_4)_4^{4-}$ to generate $Mo_2(HPO_4)_4^{2-}$ and hydrogen and present a photochemical reaction mechanism consistent with results from spectroscopic and photochemical scavenging experiments that involves the sequential one-electron photooxidation of the Mo_2 core. We believe that the proposed mechanism may be extended to accommodate the results of previous photochemical studies of other multiply bonded Mo_2O_8 dimers [e.g., $Mo_2(SO_4)_4^{4-}$, $Mo_2(aq)_x^{4+}$] in acidic solutions.

Experimental Section

General Procedures. Syntheses of the $Mo_2(II,II)$ and $Mo_2(II,III)$ phosphates were performed by using standard Schlenk-line techniques. All chemicals were reagent grade and were used as received unless otherwise noted. Phosphoric acid solutions were rigorously deoxygenated prior to use. The compounds $Cs_2Mo_2(HPO_4)_4$,[22] $K_4Mo_2Cl_8$,[23] $K_4Mo_2(SO_4)_4$,[24] and solutions of Mo_2^{4+} aquo dimer[25] were prepared by published procedures.

Syntheses. The $Mo_2(II,II)$ phosphate dimer was synthesized by ligand exchange reactions. Solutions of the dimer were prepared by three methods: (1) $K_4Mo_2Cl_8$ (0.1 g) was added to 10 mL of a 1 M H_3PO_4 solution and stirred under purified argon for 4 h; (2) 0.1 g of $K_4Mo_2(SO_4)_4$ was added with stirring to 2 M H_3PO_4 and allowed to react for 2 h; and (3) 1 mL of concentrated H_3PO_4 was added to 10 mM solutions of Mo_2^{4+} aquo dimer blanketed with argon. For each of these methods, a pink solution was obtained with a characteristic absorption band at 516 nm. Aqueous solutions of the dimer are extremely sensitive to oxygen

(1) (a) Balzani, V.; Bolletta, F.; Gandolfi, M. T.; Maestri, M. *Top. Curr. Chem.* **1978** *75*, 1–64. (b) Balzani, V.; Sabbatini, N.; Scandola, F. *Chem. Rev.* **1986**, *86*, 319–337.
(2) (a) Meyer, T. J. *Acc. Chem. Res.* **1978**, *11*, 94–100. (b) Meyer, T. J. *Prog. Inorg. Chem.* **1983**, *30*, 389–440.
(3) Sutin, N.; Creutz, C. *Adv. Chem. Ser.* **1978**, *No. 168*, 1–27.
(4) (a) Geiger, W. E.; Connelly, N. G. *Adv. Organomet. Chem.* **1985**, *24*, 87–130. (b) Geiger, W. E. *Prog. Inorg. Chem.* **1985**, *33*, 275–352. (c) Tulyathan, B.; Geiger, W. E. *J. Am. Chem. Soc.* **1985**, *107*, 5960–5967.
(5) Tsigdinos, G. A. *Top. Curr. Chem.* **1978**, *76*, 1–64.
(6) Pope, M. T. *Heteropoly and Isopoly Oxometallates*; Springer-Verlag: Berlin, 1983.
(7) Holm, R. H.; Simhon, E. D. *Molybdenum Enzymes*; Spiro, T. G., Ed.; Wiley-Interscience: New York, 1985.
(8) (a) Mann, K. R.; Lewis, N. S.; Miskowski, V. M.; Erwin, D. K.; Hammond, G. S.; Gray, H. B. *J. Am. Chem. Soc.* **1977**, *99*, 5525–5526. (b) Miskowski, V. M.; Sigal, I. S.; Mann, K. R.; Gray, H. B.; Milder, S. J.; Hammond, G. S.; Ryason, P. R. *J. Am. Chem. Soc.* **1979**, *101*, 4383–4385. (c) Gray, H. B.; Mann, K. R.; Lewis, N. S.; Thich, J. A.; Richman, R. M. *Adv. Chem. Ser.* **1978**, *No. 168*, 44–56. (d) Mann, K. R.; Gray, H. B. *Adv. Chem. Ser.* **1979**, *No. 173*, 225–235. (e) Gray, H. B.; Miskowski, V. M.; Milder, S. J.; Smith, T. P.; Maverick, A. W.; Buhr, J. D.; Gladfelter, W. L.; Sigal, I. S.; Mann, K. R. *Fundamental Research in Homogeneous Catalysis*; Tsutsui, M., Ed.; Plenum: New York, 1979; Vol. 3.
(9) (a) Caspar, J. V.; Gray, H. B. *J. Am. Chem. Soc.* **1984**, *106*, 3029–3030. (b) Marshall, J. L.; Stiegman, A. E.; Gray, H. B. *Adv. Chem. Ser.* **1986**, *No. 307*, 166–176.
(10) Roundhill, D. M. *J. Am. Chem. Soc.* **1985**, *107*, 4354–4356.
(11) Caspar, J. V. *J. Am. Chem. Soc.* **1985**, *107*, 6718–6719.
(12) Hill, C. L.; Bouchard, D. A. *J. Am. Chem. Soc.* **1985**, *107*, 5148–5157 and references therein.
(13) Cotton, F. A.; Walton, R. A. *Multiple Bonds Between Metal Atoms*; Wiley-Interscience: New York, 1982 and references therein.
(14) (a) Manning, M. C.; Trogler, W. C. *J. Am. Chem. Soc.* **1983**, *105*, 5311–5320. (b) Bursten, B. E.; Cotton, F. A.; Fanwick, P. E.; Stanley, G. G. *J. Am. Chem. Soc.* **1983**, *105*, 3082–3087. (c) Fraser, I. F.; Peacock, R. D. *Chem. Phys. Lett.* **1983**, *98*, 620–623. (d) Martin, D. S.; Huang, H.-W.; Newman, R. A. *Inorg. Chem.* **1984**, *23*, 699–701. (e) Lichtenberger, D. L.; Blevins, C. H. *J. Am. Chem. Soc.* **1984**, *106*, 1636–1641. (f) Cotton, F. A.; Wang, W. *Inorg. Chem.* **1984**, *23*, 1604–1610. (g) Huang, H.-W.; Martin, D. S. *Inorg. Chem.* **1985**, *24*, 96–101. (h) Dallinger, R. F. *J. Am. Chem. Soc.* **1985**, *107*, 7202–7204. (i) Fanwick, P. E. *Inorg. Chem.* **1985**, *24*, 258–263. (j) Fanwick, P. E.; Bursten, B. E.; Kaufmann, G. B. *Inorg. Chem.* **1985**, *24*, 1165–1169. (k) Root, D. R.; Blevins, C. H.; Lichtenberger, D. L.; Sattelberger, A. P.; Walton, R. A. *J. Am. Chem. Soc.* **1986**, *108*, 953–959. (l) Cotton, F. A.; Dunbar, K. R.; Matusz, M. *Inorg. Chem.* **1986**, *25*, 3641–3649. (m) Morris, D. E.; Sattelberger, A. P.; Woodruff, W. H. *J. Am. Chem. Soc.* **1986**, *108*, 8270–8271. (n) Hopkins, M. D.; Schaefer, W. P.; Bronikowski, M. J.; Woodruff, W. H.; Miskowski, V. M.; Dallinger, R. F.; Gray, H. B. *J. Am. Chem. Soc.* **1987**, *109*, 408–416.
(15) (a) Miskowski, V. M.; Goldbeck, R. A.; Kliger, D. S.; Gray, H. B. *Inorg. Chem.* **1979**, *18*, 86–89. (b) Winkler, J. R.; Nocera, D. G.; Netzel, T. L. *J. Am. Chem. Soc.* **1986**, *108*, 4451–4458.
(16) Nocera, D. G.; Gray, H. B. *Inorg. Chem.* **1984**, *23*, 3686–3688.
(17) (a) Zietlow, T. C.; Klendworth, D. D.; Nimry, T.; Salmon, D. J.; Walton, R. A. *Inorg. Chem.* **1981**, *20*, 947–949. (b) Tetrick, S. M.; Coombe, V. T.; Heath, G. A.; Stephenson, T. A.; Walton, R. A. *Inorg. Chem.* **1984**, *23*, 4567–4570. (c) Dunbar, K. R.; Walton, R. A. *Inorg. Chem.* **1985**, *24*, 5–10. (d) Walton, R. A. *Isr. J. Chem.* **1985**, *25*, 196–203.
(18) Chakravarty, A. R.; Cotton, F. A.; Shamshoum, E. S. *Inorg. Chem.* **1984**, *23*, 4216–4221.
(19) Cotton, F. A.; Dunbar, K. R.; Falvello, L. R.; Tomas, M.; Walton, R. A. *J. Am. Chem. Soc.* **1983**, *105*, 4950–4954.
(20) (a) Cotton, F. A.; Powell, G. L. *J. Am. Chem. Soc.* **1984**, *106*, 3371–3372. (b) Cotton, F. A.; Daniels, L. M.; Dunbar, K. R.; Falvello, L. R.; Tetrick, S. M.; Walton, R. A. *J. Am. Chem. Soc.* **1985**, *107*, 3524–3530. (c) Cotton, F. A.; Dunbar, K. R.; Price, A. C.; Schwotzer, W.; Walton, R. A. *J. Am. Chem. Soc.* **1986**, *108*, 4843–4850.
(21) Erwin, D. K.; Geoffroy, G. L.; Gray, H. B.; Hammond, G. S.; Solomon, E. I.; Trogler, W. C.; Zagars, A. A. *J. Am. Chem. Soc.* **1977**, *99*, 3620–3621.
(22) Bino, A.; Cotton, F. A. *Inorg. Chem.* **1979**, *18*, 3562–3565.
(23) Brencic, J. V.; Cotton, F. A. *Inorg. Chem.* **1970**, *9*, 351–353.
(24) Taube, H.; Bowen, A. R. *Inorg. Chem.* **1974**, *13*, 2245–2249.
(25) Bowen, A. R.; Taube, H. *J. Am. Chem. Soc.* **1971**, *93*, 3287–3289.

decomposing within minutes to dark brown uncharacterized solutions. Even in the absence of oxygen, the quadruple bond dimer slowly reacts over days to produce blue-gray solutions which exhibit a near-infrared absorption profile diagnostic of $Mo_2(HPO_4)_4^{3-}$ (vide infra). Solutions of the quadruple-bond dimer prepared by each of the three methods are contaminated inevitably with $Mo_2(HPO_4)_4^{3-}$, and accordingly, addition of K_2HPO_4 to any of the above solutions yields solid $K_4Mo_2(HPO_4)_4$ contaminated with $K_3Mo_2(HPO_4)_4$. However, addition of zinc amalgam to $Mo_2(HPO_4)_4^{4-}$ solutions smoothly converts $Mo_2(HPO_4)_4^{3-}$ to the quadruply bonded species, as evidenced by the disappearance of the near-infrared absorption band of $Mo_2(HPO_4)_4^{3-}$. In fact, stirring 2 M H_3PO_4 solutions of $K_3Mo_2(HPO_4)_4$ over zinc amalgam provides a convenient route to the preparation of pure $Mo_2(HPO_4)_4^{4-}$ solutions.

The potassium salt of $Mo_2(HPO_4)_4^{3-}$ was prepared from solutions of $Mo_2(HPO_4)_4^{4-}$. Addition of Pt foil (1 cm^2) to 25 mL of 1 M H_3PO_4 containing $Mo_2(HPO_4)_4^{4-}$ (0.4 mmol) quantitatively yields $Mo_2(HPO_4)_4^{3-}$ in 2 h. Dropwise addition of a saturated solution of K_2HPO_4 leads to the immediate precipitation of a fine blue-gray powder. The product was filtered under vacuum and washed with three 5-mL portions of 2 M H_3PO_4 at 0 °C. Aliquots for all washings were delivered by cannula. The solid was dried and stored under vacuum. Alternatively, a more facile route to the mixed-valence dimer involved the addition of 0.505 g of $K_4Mo_2Cl_8$ (0.800 mmol) to 15 mL of degassed 1 M H_3PO_4. After the solution was stirred at room temperature for 1 h under argon, 0.108 g of $K_2S_2O_8$ (0.400 mmol) was added to the solution via a sample charger. The red solution quickly turned blue, and a blue-gray powder precipitated from the solution. The solid was collected by using Schlenk-line techniques. Anal. Calcd (Found) for $K_3Mo_2H_4P_4O_{16}$: Mo, 27.68 (27.60). Solids and solutions of the mixed-valence dimer are sensitive to oxygen, but the compound is indefinitely stable under inert atmospheres.

Instrumentation and Procedures. EPR spectra were recorded by using a Bruker ER 200D X-band spectrometer equipped with an Oxford ESR-9 liquid-helium cryostat. Magnetic fields were measured with a Bruker ER035M gaussmeter, and frequencies were measured with a Hewlett-Packard 5245L frequency counter. Magnetic susceptibility measurements were made with a SHE 800 series variable-temperature SQUID magnetometer.

Absorption spectra were recorded with a Cary 17D spectrophotometer. Extinction coefficients were determined in high-vacuum cells consisting of a 1-cm quartz cuvette and a 10-mL side arm. These two chambers were separated by two high-vacuum Konte quick-release Teflon stopcocks. For measurements of molar absorptivity coefficients, known volumes of phosphoric acid were pipetted into the side arm and subjected to five freeze–pump–thaw cycles before mixing with weighed samples of solid $K_3Mo_2(HPO_4)_4$ contained in the cuvette cell. Known concentrations of solutions of $Mo_2(HPO_4)_4^{4-}$ were prepared by zinc amalgam reduction of $Mo_2(HPO_4)_4^{3-}$ solutions. Extinction coefficients were calculated from Beer–Lambert plots composed of at least seven points.

The thermal reaction of $Mo_2(HPO_4)_4^{4-}$ in 2 M H_3PO_4 was monitored following the intensities of the $\delta \rightarrow \delta^*$ absorption bands of $Mo_2(HPO_4)_4^{3-}$ and $Mo_2(HPO_4)_4^{4-}$. Hydrogen was quantitatively determined by Toepler pumping the gas above reacted solutions through two liquid-nitrogen traps into a calibrated volume and manometrically measuring the pressure.

Resonance Raman spectra were recorded with a Spex 1401 double monochromator and associated Ramalog electronics. A Spectra Physics 165 argon ion laser was the excitation source, and incident powers were 20–40 mW. All spectra were collected at a 90° scattering geometry from solid samples at room temperature.

Electrochemical measurements were made with a PAR Model 173 potentiostat, 175 universal programmer, 179 digital coulometer, and a Houston Instruments Model 2000 X-Y chart recorder. Cyclic voltammetry was performed at 22 ± 2 °C by using a conventional H-cell design and a three-electrode system consisting of a polished glassy carbon working electrode (A = 0.08 cm^2), a Pt wire auxiliary electrode, and a saturated calomel reference electrode.

Sample irradiations were performed by using a Hanovia 1000-W Hg/Xe high-pressure lamp. The beam was collimated and passed through a 10-cm circulating water filter. Photolyses experiments were performed in two-arm evacuable cells equipped with Kontes quick-release Teflon values. Sample temperatures were thermostated at 10.0 ± 0.5 °C in all photochemical experiments. Gas chromatographic analyses of hydrogen and nitrogen above reacted solutions were obtained with a Hewlett-Packard 5710A gas chromatograph equipped with a 100/200 carbosieve S-II column. Quantum yields for the disappearance of $Mo_2(HPO_4)_4^{3-}$ were measured at 254, 313, and 367 nm by using ferrioxalate actinometry. Excitation wavelengths were isolated with standard solution filters. Visible irradiations were accomplished by using colored glass high-energy cutoff filters from Schott.

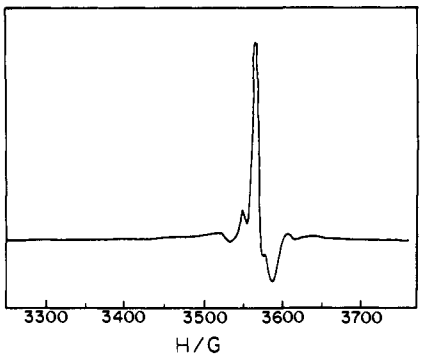

Figure 1. X-band (9.460-GHz) ESR spectrum of a frozen solution of $K_3Mo_2(HPO_4)_4$ in 7.5 M H_3PO_4 at 5 K.

Results and Discussion

Magnetic and Spectroscopic Characterization of $Mo_2(HPO_4)_4^{n-}$ (n = 2–4) Species. A central result to emerge from exhaustive spectroscopic studies of multiply bonded metal–metal dimers is a consistent description of the electronic structure of these complexes in terms of a σ, π, and δ molecular orbital framework.[13,26] One consequence of this model is the prediction that dimers of bond orders 4 ($\sigma^2\pi^4\delta^2$) and 3 ($\sigma^2\pi^4$) will possess a diamagnetic ground state while mixed-valence dimers of bond order 3.5 ($\sigma^2\pi^4\delta^1$) will be paramagnetic. We were interested in investigating the magnetic properties of $Mo_2(HPO_4)_4^{3-}$ and $Mo_2(HPO_4)_4^{4-}$ because these studies in connection with a previous susceptibility measurement on the pyridinium salt of $Mo_2(HPO_4)_4^{2-}$,[27] which was shown to be diamagnetic, would provide magnetic data on the first homologous M$\overset{n}{-}$M series possessing a $\sigma^2\pi^4\delta^n$ (n = 0–2) ground-state configuration.

The predicted paramagnetic behavior of $Mo_2(HPO_4)_4^{3-}$ is confirmed by magnetic susceptibility measurements of solids from 5 to 300 K at a field of 5500 G. The temperature dependence of the magnetic susceptibility follows Curie law behavior, and the magnetic moment of $K_3Mo_2(HPO_4)_4$ is 1.58 μ_B. Correction for the diamagnetic contribution to the magnetic moment was provided by the room-temperature magnetic susceptibility of the pyridinium salt of $Mo_2(HPO_4)_4^{2-}$. In accordance with susceptibility results, EPR spectra of frozen solutions of $K_3Mo_2(HPO_4)_4$ at 5 K (Figure 1) show a paramagnetic species in an axial environment, $g_\perp$ = 1.894 and $g_\parallel$ = 1.886. As described in detailed EPR studies of $Mo_2(SO_4)_4^{3-}$[28] and other M$\overset{3.5}{-}$M dimers,[29] the EPR signal reproduced in Figure 1 is consistent with a species in which the unpaired electron is coupled between two equivalent molybdenum nuclei.

Reduction of $Mo_2(HPO_4)_4^{3-}$ by one electron will yield a quadruply bonded complex which should exhibit rigorous diamagnetism. Unfortunately, the accurate determination of the magnetic susceptibility of $Mo_2(HPO_4)_4^{4-}$ is precluded by our inability to cleanly isolate salts of the quadruple-bond complex from the mixed-valence dimer. Indeed, EPR spectra of solid samples of $K_4Mo_2(HPO_4)_4$ at 5 K show signals identical with that of $K_3Mo_2(HPO_4)_4$. That the intensity of the signal varies with sample preparation indicates that the observed paramagnetism arises from $Mo_2(HPO_4)_4^{3-}$ impurities and no evidence for a distinct EPR signal attributable to $Mo_2(HPO_4)_4^{4-}$ can be discerned. Thus, to the best of our knowledge, the magnetic properties of the Mo_2 phosphate series are accommodated by the electronic structure model of M$\overset{n}{-}$M (D_{4h}) dimers.

Solids and solutions of $Mo_2(HPO_4)_4^{4-}$ are pink in color. Figure 2 displays the electronic absorption spectrum of the dimer in 2

(26) Trogler, W. C.; Gray, H. B. *Acc. Chem. Res.* **1978**, *11*, 232–239.
(27) Hopkins, M. D.; Miskowski, V. M.; Gray, H. B. *J. Am. Chem. Soc.* **1986**, *108*, 959–963.
(28) Cotton, F. A.; Frenz, B. A.; Pedersen, E.; Webb, T. R. *Inorg. Chem.* **1975**, *14*, 391–398.
(29) (a) Cotton, F. A.; Pedersen, E. *Inorg. Chem.* **1975**, *14*, 388–391. (b) Cotton, F. A.; Pedersen, E. *J. Am. Chem. Soc.* **1975**, *97*, 303–308.

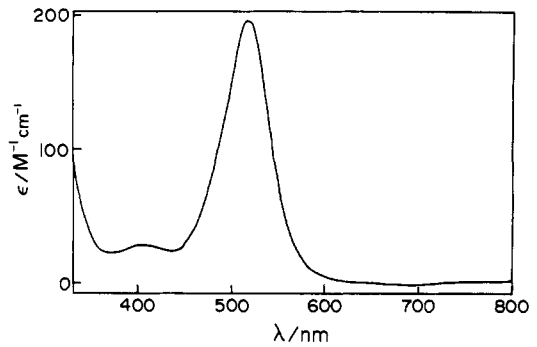

Figure 2. Electronic absorption spectrum of $Mo_2(HPO_4)_4^{4-}$ ion in 2 M H_3PO_4 at room temperature.

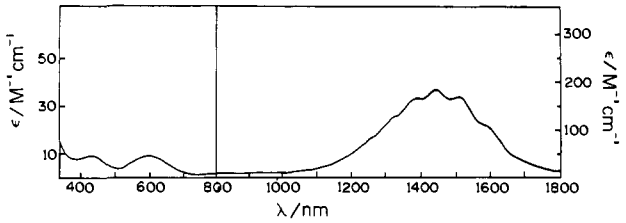

Figure 3. Electronic absorption spectrum of $K_3Mo_2(HPO_4)_4$ in 2 M H_3PO_4 at 25 °C.

M H_3PO_4. The lowest energy absorption band (λ_{max} = 516 nm (ϵ = 196 M^{-1} cm^{-1})) is comparable in energy and intensity to that of $Mo_2(SO_4)_4^{4-}$ and by analogy is assigned to the $\delta^2 \rightarrow \delta\delta^*$ transition. As expected for a dipole-allowed transition, the band sharpens upon cooling solutions to 77 K, but the integrated intensity of the band remains constant; the absorption profile remains vibrationally featureless at low temperature. In addition to the $\delta^2 \rightarrow \delta\delta^*$ transition, visible and ultraviolet absorption systems in $Mo_2(HPO_4)_4^{4-}$ have direct analogues in $Mo_2(SO_4)_4^{4-}$ spectra. The absorption (λ_{max} = 408 nm (ϵ = 27 M^{-1} cm^{-1})) immediately to higher energy of the $\delta^2 \rightarrow \delta\delta^*$ transition is especially noteworthy; a similarly positioned band in $Mo_2(SO_4)_4^{4-}$ has tentatively been assigned to the $\pi \rightarrow \delta^*$ transition.[27]

The electronic absorption spectrum of $Mo_2(HPO_4)_4^{3-}$ (Figure 3) is dominated by a prominent absorption profile in the near-infrared (λ_{max} = 1438 nm (ϵ = 180 M^{-1} cm^{-1})) and two weak visible bands at 595 (ϵ = 10 M^{-1} cm^{-1}) and 420 nm (ϵ = 8 M^{-1} cm^{-1}). Similar to the quadruple-bond dimers, the spectra of Mo_2(II,III) sulfate and phosphate are nearly identical. The results of previous spectroscopic studies of $Mo_2(SO_4)_4^{3-}$ are consistent with assignment of the near-infrared absorption band to the $\delta \rightarrow \delta^*$ ($^2B_{1u} \leftarrow {}^2B_{2g}$) transition.[21,30] This significant red-shift of the $\delta \rightarrow \delta^*$ transition in mixed-valence Mo_2 dimers is explained by the absence of two-electron term contributions to the transition energy for $\sigma^2\pi^4\delta^1$ configured ground-state species. Similar to $Mo_2(SO_4)_4^{3-}$ ion, the $\delta \rightarrow \delta^*$ absorption band of $Mo_2(HPO_4)_4^{3-}$ exhibits a vibrational progression in solution at room temperature. As shown in Figure 4, the vibrational peaks sharpen considerably upon cooling the phosphoric acid solution to 77 K. The 334 cm^{-1} spacing is consistent with a progression in the symmetric metal–metal stretching vibration.

With regard to the visible absorption profile of $Mo_2(HPO_4)_4^{3-}$, the analogous absorption bands at 417 and 595 nm in $Mo_2(SO_4)_4^{3-}$ have been assigned by Hopkins et al. to the $\pi \rightarrow \delta^*$ and $\pi \rightarrow \delta$ transitions, respectively. These assignments, which resulted from a comparative analysis of Mo_2(II,II) and Mo_2(II,III) sulfate and Mo_2(III,III) phosphate spectra, are predicated on the assumption that bridging SO_4^{2-} and HPO_4^{2-} ligands will perturb the electronic structure of a Mo_2 core in a similar fashion. In this context, the absorption spectra of the homologous Mo_2 phosphate series reported herein confirm this contention and accordingly support the $\pi \rightarrow \delta$ and $\pi \rightarrow \delta^*$ assignments for the visible absorption bands

(30) Fanwick, P. E.; Martin, D. S.; Webb, T. R.; Robbins, G. A.; Newman, R. A. *Inorg. Chem.* **1978**, *17*, 2723–2727.

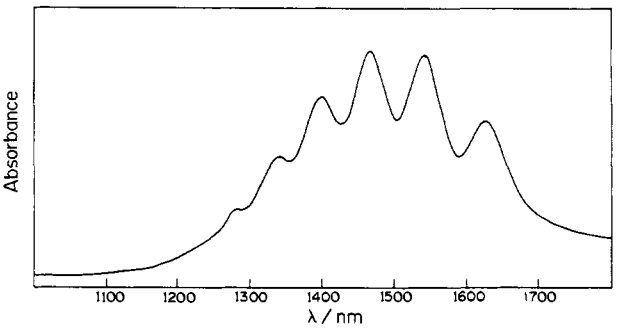

Figure 4. Near-infrared absorption band of $K_3Mo_2(HPO_4)_4$ in a frozen phosphoric acid solution at 77 K.

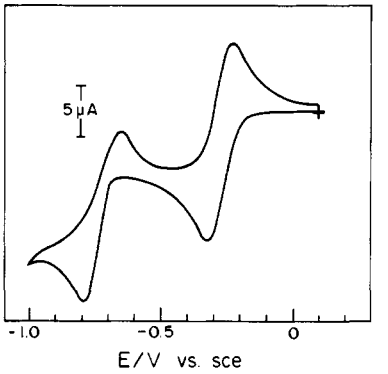

Figure 5. Cyclic voltammogram of a 2.5 mM solution of the pyridinium salt of $Mo_2(HPO_4)_4^{2-}$ in 2 M H_3PO_4. The working electrode was glassy carbon (A = 0.08 cm^2), and the scan rate was 2 mV s^{-1}.

of $Mo_2(HPO_4)_4^{3-}$ and $Mo_2(SO_4)_4^{3-}$.

Raman spectra of solid samples of $Mo_2(HPO_4)_4^{n-}$ (n = 2–4) at room temperature were recorded with 4880-Å excitation light. The excitation frequency falls within the contour of the metal-localized absorption profiles and significant enhancement of Raman peaks associated with metal–metal vibrations can be expected.[31] Prominent bands are observed at 345, 352, and 356 cm^{-1} in the Raman spectra of Mo_2(II,II), Mo_2(II,III), and Mo_2(III,III) phosphate, respectively; this latter frequency is in excellent agreement with a previous study of $Mo_2(HPO_4)_4^{2-}$ in which a band at 358 cm^{-1} was attributed to ν(Mo–Mo).[27] Assignment of the observed bands in the Mo_2 phosphate series to ν(Mo–Mo) is consistent with their frequencies which fall squarely within the 350–400 cm^{-1} range which characterizes metal–metal vibrations in Mo^{n}–Mo dimers and is also supported by the presence of energetically similar peaks in Mo_2 sulfate dimers.[32] Given the ν(Mo–Mo) assignment, a striking result of $Mo_2(HPO_4)_4^{n-}$ (n = 2–4) Raman spectra is the observed increase in metal–metal stretching frequency with decreasing bond order. Precedent for this puzzling trend has heretofore existed as an anomaly in the Raman spectra of Mo_2(II,II) (ν(Mo–Mo) = 371 cm^{-1}) and Mo_2(II,III) (ν(Mo–Mo) = 373, 386 cm^{-1}) sulfate. An explanation for this apparent inconsistency is the ability of the bridging ligand to modulate the metal–metal frequency,[33] although the origin of this effect has not clearly been established. Nevertheless, the Raman results of the phosphate and sulfate series clearly demonstrate the ability of bridging ligands to vitiate predictions using simple bond order arguments.

Oxidation–Reduction Chemistry. The cyclic voltammogram of $Mo_2(HPO_4)_4^{2-}$ in 1 M H_3PO_4, shown in Figure 5, exhibits two oxidation processes. Reversible electrochemical behavior is sug-

(31) (a) Clark, R. J. H.; Franks, M. L. *J. Am. Chem. Soc.* **1975**, *97*, 2691–2697. (b) Clark, R. J. H.; Stead, M. J. *Inorg. Chem.* **1983**, *22*, 1214–1220.

(32) (a) Angell, C. L.; Cotton, F. A.; Frenz, B. A.; Webb, T. R. *J. Chem. Soc., Chem. Commun.* **1973**, 399–400. (b) Reference 13, Chapter 8.

(33) Loewenschuss, A.; Shamir, J.; Ardon, M. *Inorg. Chem.* **1976**, *15*, 238–241.

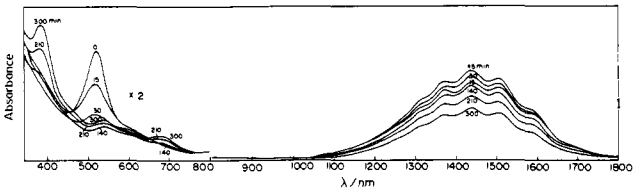

Figure 6. Electronic absorption spectral changes during irradiation ($\lambda \geq 335$ nm) of $Mo_2(HPO_4)_4^{4-}$ in 2 M D_3PO_4. Due to spectral congestion in the visibile spectral region, the 45-min trace is not illustrated between 350 and 800 nm. The absorbance sensitivity in the visible spectral region is twice that of the infrared spectral region.

gested by linear plots of the cathodic and anodic currents vs. $\nu^{1/2}$ (scan rate, ν: 5–100 mV s^{-1}), and values of 0.98 ± 0.04 for ratios of the anodic and cathodic peak currents.[34] The identities of these two electrode processes are revealed by electrochemical experiments on solutions of the quadruply bonded and mixed-valent phosphate dimers. Cyclic voltammograms identical with the one displayed in Figure 5 are observed upon scanning the electrode potential from the appropriate resting potentials of solutions of Mo_2(II,II) and Mo_2(II,III) phosphate. These results lead us to assign the waves at −0.25 and −0.67 V vs. SCE to the $Mo_2(HPO_4)_4^{2-/3-}$ and $Mo_2(HPO_4)_4^{3-/4-}$ couples, respectively.

The syntheses of Mo_2 phosphate dimers and their reaction chemistry are easily understood in the context of the above electrochemical results. Our observation that solids of $Mo_2(HPO_4)_4^{4-}$ precipitated from acidic solutions are inevitably contaminated with $Mo_2(HPO_4)_4^{3-}$ is consistent with the negative potential of the $Mo_2(HPO_4)_4^{3-/4-}$ couple with respect to the standard hydrogen electrode. Indeed $Mo_2(HPO_4)_4^{4-}$ in 2 M H_3PO_4 solution slowly converts to $Mo_2(HPO_4)_4^{3-}$ as evidenced by the disappearance of the $^1(\delta^2 \rightarrow \delta\delta^*)$ absorption band at 516 nm and the concomitant growth of the $^2(\delta \rightarrow \delta^*)$ absorption of $Mo_2(HPO_4)_4^{3-}$. Closer analysis of the reaction reveals the quantitative conversion of quadruple-bond dimer to mixed-valence species ($\tau_{1/2}$ = 27.5 h) and chromatographic analysis identifies hydrogen as a reaction product.[35] Toepler pumping the gas above completely reacted solutions reveals that 0.39 mol of H_2/mol of $K_4Mo_2(HPO_4)_4$ is evolved, thereby establishing the overall reaction stoichiometry as

$$Mo_2(HPO_4)_4^{4-} + H^+ \rightarrow Mo_2(HPO_4)_4^{3-} + {}^1/_2H_2 \quad (1)$$

Reduction of protons to hydrogen radicals is a highly energetic process [$E(H^+/H)$ = 2.6 V vs. SCE],[36] and hence, direct reaction of the quadruple bond dimer with H^+ to produce the mixed-valence dimer is not thermodynamically feasible. We propose that $Mo_2(HPO_4)_4^{4-}$ reacts in acidic solution to $Mo_2(HPO_4)_4^{2-}$ which then reacts in a comproportionation reaction to produce mixed-valence dimer according to the following scheme:

$$Mo_2(HPO_4)_4^{4-} + 2H^+ \rightarrow Mo_2(HPO_4)_4^{2-} + H_2 \quad (2)$$

$$Mo_2(HPO_4)_4^{4-} + Mo_2(HPO_4)_4^{2-} \rightarrow 2Mo_2(HPO_4)_4^{3-} \quad (3)$$

Consistent with this scheme is our observation that addition of a phosphoric acid solution of $Mo_2(HPO_4)_4^{2-}$ to one of $Mo_2(HPO_4)_4^{4-}$ leads to the immediate and quantitative production of $Mo_2(HPO_4)_4^{3-}$. In view of previous studies on $M\overset{n}{-}M$ dimers which have demonstrated large rate constants for electron exchange reactions involving δ orbitals,[37] the facility of reaction 3 is not surprising since the comproportionation simply involves the transfer of an electron between the δ orbitals of the Mo_2 phosphato dimers. We therefore believe that the slow thermal conversion of $Mo_2(HPO_4)_4^{4-}$ to $Mo_2(HPO_4)_4^{3-}$ in phosphoric acid solutions, in the context of the above scheme, is a consequence of large kinetic barriers associated with reaction 2.

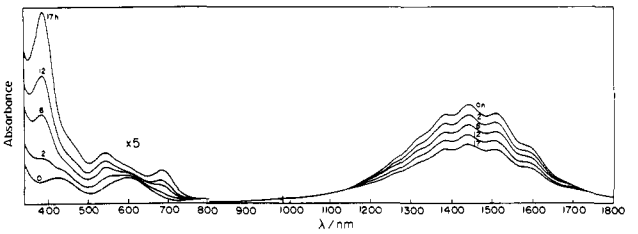

Figure 7. Absorption changes resulting from irradiating ($\lambda \geq 335$ nm) 2 M D_3PO_4 solutions of $Mo_2(HPO_4)_4^{3-}$. The visible absorbance scale is 5 times greater than the near-infrared absorbance scale.

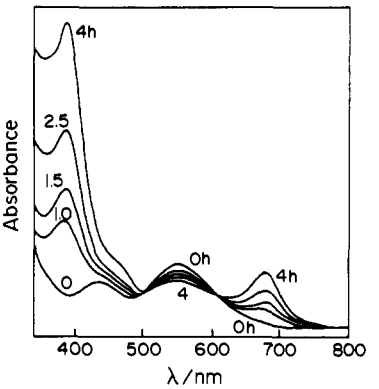

Figure 8. Spectral changes during irradiation ($\lambda \geq 335$ nm) of $Mo_2(HPO_4)_4^{2-}$ in 2 M D_3PO_4. No absorption bands appear in the near-infrared spectral region during the photolysis reaction.

Photochemistry. In striking contrast to the slow thermal chemistry, reaction of $Mo_2(HPO_4)_4^{4-}$ in acidic solution is markedly accelerated by ultraviolet irradiation. Spectral changes for the room-temperature irradiation ($\lambda \geq 335$ nm) of $Mo_2(HPO_4)_4^{4-}$ in 2 M D_3PO_4 are shown in Figure 6. An initial decrease in the intensity of the $\delta^2 \rightarrow \delta\delta^*$ absorption band of $Mo_2(HPO_4)_4^{4-}$ is accompanied by an increase in the $\delta \rightarrow \delta^*$ absorption of $Mo_2(HPO_4)_4^{3-}$. Ensuing reaction of the mixed-valence dimer is revealed by the disappearance of the near-infrared $\delta \rightarrow \delta^*$ absorption. A series of weak changes in the visible region is observed with continued irradiation, and the photolysis reaction terminates with an absorption profile distinguished by a strong absorption band at 385 nm and a weaker band at 685 nm. The absence of an isosbestic point during the photolysis reaction and the growth and decay of the characteristic near-infrared band of $Mo_2(HPO_4)_4^{3-}$ are consistent with a multistep photooxidation pathway with subsequent reaction of the Mo_2 primary photoproduct.

Further analysis of the $Mo_2(HPO_4)_4^{4-}$ photoreaction was pursued with investigations of the photochemistry of Mo_2(II,III) and Mo_2(III,III) phosphate dimers. Irradiation ($\lambda \geq 335$ nm) of $Mo_2(HPO_4)_4^{3-}$ in 2 M D_3PO_4 produces the spectral changes illustrated in Figure 7. The intensity of the near-infrared band of $Mo_2(HPO_4)_4^{3-}$ monotonically decreases, and bands at 420 and 540 nm appear during the initial stages of irradiation. With continued irradiation, the 540-nm band disappears and absorptions grow in at 385 and 690 nm. This latter spectrum is identical with the terminating spectrum of $Mo_2(HPO_4)_4^{4-}$ photolysis. The quantum yield for the disappearance of $Mo_2(HPO_4)_4^{3-}$ is 0.046 (λ_{exc} = 313 nm) whereas no reaction is observed for solutions of the mixed-valence dimer stored in the dark at room temperature.

The appearance of the 540-nm band during the early stages of $Mo_2(HPO_4)_4^{3-}$ photolysis is consistent with the formation of

(34) Bard, A. J.; Faulkner, L. R. *Electrochemical Methods. Fundamentals and Applications*; Wiley-Interscience: New York, 1980.

(35) Quantitative rate measurements for the disappearance of $Mo_2(HPO_4)_4^{4-}$ is precluded by our inability to prepare solid $K_4Mo_2(HPO_4)_4$. While pure solutions of $Mo_2(HPO_4)_4^{4-}$ can be obtained by stirring over Zn/Hg, these solutions, when isolated from the amalgam, react at rates accelerated to those observed for solutions of $Mo_2(HPO_4)_4^{4-}$ which are not exposed to Zn/Hg. These data suggest that conversion of $Mo_2(HPO_4)_4^{4-}$ to $Mo_2(HPO_4)_4^{3-}$ is catalyzed by Zn^{2+}. Consistent with reactions 2 and 3 in the text (vide infra), the equilibrium $Mo_2(HPO_4)_4^{4-} + Zn^{2+} \rightleftharpoons Mo_2(HPO_4)_4^{2-} + Zn$ will be driven to the right by the comproportionation reaction between $Mo_2(HPO_4)_4^{4-}$ and $Mo_2(HPO_4)_4^{2-}$ to produce $Mo_2(HPO_4)_4^{3-}$.

(36) Baxendale, J. H. *Rad. Res. Suppl.* **1964**, *4*, 139–140.

(37) Nocera, D. G.; Gray, H. B. *J. Am. Chem. Soc.* **1981**, *103*, 7349–7350.

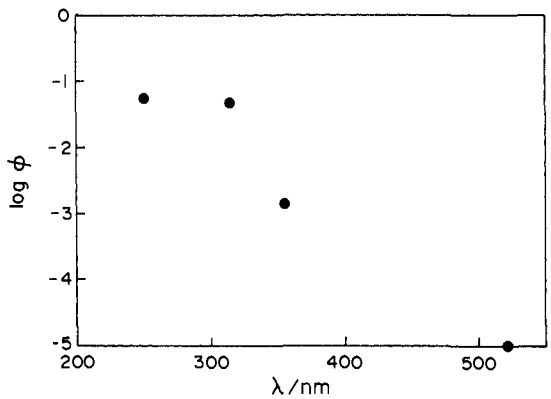

Figure 9. Action spectrum for the photolysis reaction: $Mo_2(HPO_4)_4^{3-} + H^+ \rightarrow Mo_2(HPO_4)_4^{2-} + {}^1/_2H_2$. Quantum yields were measured by monitoring the $\delta \rightarrow \delta^*$ absorption band of $Mo_2(HPO_4)_4^{3-}$.

$Mo_2(HPO_4)_4^{2-}$ as a primary photoproduct. Support for this contention is provided by the photochemistry of $Mo_2(HPO_4)_4^{2-}$. Figure 8 displays the absorption changes accompanying irradiation ($\lambda \geq 335$ nm) of 2 M D_3PO_4 solutions of $Mo_2(HPO_4)_4^{2-}$. Smooth conversion of $Mo_2(HPO_4)_4^{2-}$ to the photoproduct characterized by the 385- and 685-nm absorptions is observed, and in contrast to Mo_2(II,II) and Mo_2(II,III) photochemistry, isosbestic points at 500 and 608 nm attest to a stoichiometric photoreaction. While the identity of this ubiquitous photoproduct has not yet been revealed, a clue to its identity is provided by gas chromatographic analysis. The detection of hydrogen as a photolysis byproduct suggests that the Mo_2(III,III) core is photooxidized. More detailed investigations to determine the photoproduct and $Mo_2(HPO_4)_4^{2-}$ photoreaction mechanism will be reported in a separate study.

The above photochemical results of $Mo_2(HPO_4)_4^{n-}$ (n = 2–4) dimers substantiate a sequential oxidation pathway. The relatively complicated series of spectral changes induced by irradiation of $Mo_2(HPO_4)_4^{4-}$ solutions are explained by a reaction scheme in which the final photoproduct (λ_{max} = 385 and 685 nm) is generated directly from $Mo_2(HPO_4)_4^{2-}$, which in turn is a primary photoproduct of $Mo_2(HPO_4)_4^{3-}$ which is the primary photoproduct of irradiated solutions of $Mo_2(HPO_4)_4^{4-}$. Gas chromatography reveals a concomitant production of hydrogen with each of these discrete dimer photoprocesses. A reaction sequence accommodating these observations is as follows:

$$Mo_2(HPO_4)_4^{4-} \xrightarrow[h\nu\,(\lambda > 335\text{ nm})]{H^+} {}^1/_2H_2$$

$$Mo_2(HPO_4)_4^{3-} \xrightarrow[h\nu\,(\lambda > 335\text{ nm})]{H^+} Mo_2(HPO_4)_4^{2-} + {}^1/_2H_2 \quad (4)$$

As previously noted, ensuing $Mo_2(HPO_4)_4^{2-}$ photooxidation leads to the generation of a presently undetermined higher valent molybdenum species and hydrogen. Thus the overall photochemical reaction corresponds to a multielectron process which involves the exchange of at least two electrons.

Insight into the nature of the photoactive state of the Mo_2 phosphate systems is provided by the wavelength dependences of $Mo_2(HPO_4)_4^{n-}$ (n = 2–4) photoprocesses. The photochemistry of each of the Mo_2 phosphate systems is inhibited as the irradiation wavelength is increased. Illustrative of this reactivity trend is the photooxidation reaction of $Mo_2(HPO_4)_4^{3-}$ which proceeds promptly with ultraviolet irradiation but is suppressed upon shifting the excitation wavelength into the visible spectral region; Figure 9 summarizes the wavelength dependence of the reaction quantum yield. No photoreaction can be detected when $Mo_2(HPO_4)_4^{3-}$ solutions are irradiated at wavelengths longer than 475 nm. Between 300 and 400 nm, the quantum yield increases monotonically with decreasing irradiation wavelengths. And for wavelengths less than 300 nm, the quantum yield asymptotically approaches a limiting value of 0.05. Similarly, facile conversion of $Mo_2(HPO_4)_4^{4-}$ is observed for excitation wavelengths less than 367 nm, whereas solutions of $Mo_2(HPO_4)_4^{4-}$ do not photoreact with irradiation into the ${}^1(\delta^2 \rightarrow \delta\delta^*)$ absorption band. These results imply that the photoreactivity of the Mo_2 phosphate dimers is not associated with the lowest energy metal localized transition of the Mo_2 core but rather with high-energy excited states that lie in the ultraviolet spectral region.

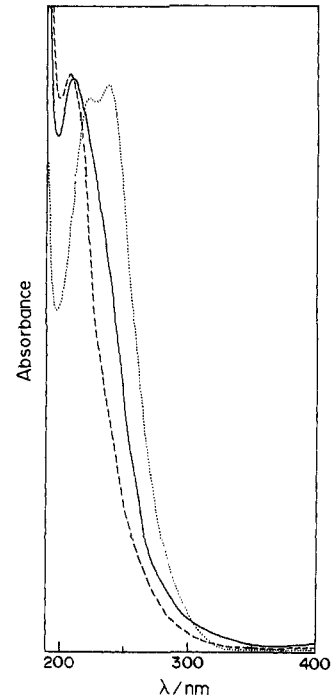

Figure 10. Ultraviolet absorption bands of $K_4Mo_2(HPO_4)_4$ (---), $K_3Mo_2(HPO_4)_4$ (—), and $K_2Mo_2(HPO_4)$ (···) in 2 M H_3PO_4 at 25 °C.

In an effort to identify these high-energy photoactive excited states, we recorded the ultraviolet absorption spectra of the Mo_2 phosphato complexes in 2 M H_3PO_4. As illustrated in Figure 10, a prominent absorption band dominates the ultraviolet spectral region of the three phosphato dimers ($\lambda_{max}(Mo_2(HPO_4)_4^{4-})$ = 206 nm; $\lambda_{max}(Mo_2(HPO_4)_4^{3-})$ = 210 nm; $\lambda_{max}(Mo_2(HPO_4)_4^{2-})$ = 220 nm). The relative insensitivity of the band maximum to the oxidation state of the Mo_2 core suggests that the transition is metal-localized. Theoretical calculations predict that the allowed $\pi \rightarrow \pi^*$ transition of $M\underline{\underline{^n}}M$ dimers should be observed in the ultraviolet energy region[38] and polarized absorption spectroscopic studies[39] support this contention. Accordingly, we assign the 206-nm absorption of $Mo_2(HPO_4)_4^{4-}$ to the $\pi \rightarrow \pi^*$ transition. The modest red-shift of the band across the Mo_2(II,II), Mo_2(II,III), and Mo_2(III,III) series is consistent with a concomitant decrease in the metal–metal interaction.[40] An additional absorption band is observed at 237 nm for Mo_2(III,III) phosphate. That this absorption is not present at lower energies in the spectra of Mo_2(II,III) and Mo_2(II,II) phosphato dimers precludes its assignment to a transition corresponding to oxidation of the metal core, such as charge-transfer-to-solvent (CTTS), because absorption bands attributable to transitions of this type would exhibit a marked red-shift with reduction of the metal core. Conversely, the absence of this band in Mo_2(II,II) and Mo_2(II,III) phosphate

(38) (a) Norman, J. G., Jr.; Kolari, H. J. *J. Chem. Soc., Chem. Commun.* **1974**, 303–305. (b) Norman, J. G., Jr.; Kolari, H. J. *J. Am. Chem. Soc.* **1975**, *97*, 33–37. (c) Hay, P. J. *J. Am. Chem. Soc.* **1982**, *104*, 7007–7017. (d) Mathisen, K. B.; Wahlgren, U.; Pettersson, L. G. M. *Chem. Phys. Lett.* **1984**, *104*, 336–342. (e) Stromberg, A.; Pettersson, L. G. M.; Wahlgren, U. *Chem. Phys. Lett.* **1985**, *118*, 389–394.

(39) Mortola, A. P.; Moskowitz, J. W.; Rosch, N.; Cowman, C. D.; Gray, H. B. *Chem. Phys. Lett.* **1975**, *32*, 283–286.

(40) Crystal structures of $Mo_2(HPO_4)_4^{2-}$ [22] and $Mo_2(SO_4)_4^{n-}$ (n = 3 and 4, ref 28) reveal that the metal–metal distance increases by ~0.06 Å per δ electron.

spectra is presumably due its a blue-shift into the hard ultraviolet, thereby suggesting that the transition exhibits significant LMCT character. Thus, although the $\pi\pi^*$ and LMCT excited states of the Mo_2(III,III) dimer are potentially photoactive, our inability to detect charge-transfer excited states in the 200–250 nm region for the Mo_2(II,II) and Mo_2(II,III) phosphato complexes implies that the photoreactivity of these species is derived exclusively from $\pi \rightarrow \pi^*$ excitation.

In an effort to ascertain the nature of the intermediates leading to hydrogen production, we photolyzed solutions of $Mo_2(HPO_4)_4^{4-}$ and $Mo_2(HPO_4)_4^{3-}$ under atmospheres of N_2O, which is an effective trap of highly energetic radical intermediates. Ultraviolet irradiation ($\lambda \geq 335$ nm) of $Mo_2(HPO_4)_4^{4-}$ and $Mo_2(HPO_4)_4^{3-}$ in N_2O-saturated 2 M H_3PO_4 solutions yields the one-electron photooxidized Mo_2 phosphato complex and N_2. These results are consistent with the generation of H atoms as a primary photoproduct of $\pi \rightarrow \pi^*$ excitation of Mo_2 phosphato dimers because nitrogen, which is generated at the expense of hydrogen formation, is a product expected from the reaction of hydrated hydrogen atoms with N_2O.[41,42] Annihilation of two hydrogen atoms or subsequent oxidation of the starting complex by a hydrogen atom to yield H^- followed by a facile proton trapping reaction will result in hydrogen production.

The smooth conversion of Mo_2(II,II) phosphate to Mo_2(III,III) phosphate dimer with the concomitant production of hydrogen clearly demonstrates the capacity of the $M\underline{^n}M$ core to engender multielectron photochemical transformations by coupling the oxidation–reduction chemistry of the two metal centers along a controlled reaction pathway. It is evident from the reduction potentials of the Mo_2 phosphato complexes that the overall reaction is thermodynamically favored and hence the stabilities of the $Mo_2(HPO_4)_4^{4-}$ and $Mo_2(HPO_4)_4^{3-}$ ions in H_3PO_4 must necessarily arise from large kinetic barriers associated with oxidation of the Mo_2 cores. Our results demonstrate that these barriers are easily surmounted along photochemical reaction pathways. Our $\pi \rightarrow \pi^*$ assignment of the photoactive state of Mo_2 phosphato complexes conforms with the general reactivity pattern which has developed for $M\underline{^n}M$ dimers in acidic solution. Namely, low-energy metal-localized excited states are not responsible for the photooxidation chemistry of $M\underline{^n}M$ dimers in protic environments. We believe that the proposed photochemical mechanism is not specific to Mo_2 phosphato complexes but may be extended to accommodate the photochemistry of other Mo_2O_8 complexes in acidic solution.[44] For instance, the electronic absorption spectra of $Mo_2(SO_4)_4^{3-}$ and $Mo_2(SO_4)_4^{4-}$ are completely analogous to the spectra of the corresponding Mo_2 phosphato complexes in that an intense absorption band whose energy is independent of the oxidation state of the Mo_2 core (λ_{max} = 239 and 235 nm for $Mo_2(SO_4)_4^{3-}$ and $Mo_2(SO_4)_4^{4-}$, respectively) dominates the ultraviolet region. These data support assignment of the band to a $\pi \rightarrow \pi^*$ transition, and it is reasonable to propose that the photoreactivity of the $Mo_2(SO_4)_4^{4-}$ system, similar to the phosphato series, originates from $\pi \rightarrow \pi^*$ excitation. The two-electron photochemistry of the Mo_2 phosphate system, as opposed to the one-electron transformations of the sulfate system, reflects the increased susceptibility of the Mo_2 core toward oxidation when ligated by phosphate. This difference between the oxidation–reduction properties of Mo_2 phosphato and sulfato complexes may derive from the fact that the ligands of the former complex possess a dissociable proton. In this connection, phosphoric acid and its ions exhibit enhanced proton ionization upon coordination to a metal; and ionization is enhanced further when the ions chelate a metal center.[45,46] In view of the relatively high charge of the Mo_2 core and the bridging coordination geometry of phosphate, a significantly reduced interaction of the proton with the oxygens of PO_4^{3-} may be expected. Weak or complete dissociation of a proton from one or more of the HPO_4^{2-} ligands will increase the overall negative charge of the complex and facilitate oxidation of the Mo_2 core.[47] This ability of the phosphate ion to significantly shift the oxidation potential of metal cores to more positive values presages unique photooxidation chemistry of transition-metal phosphates. We are extending investigations to a variety of metal–metal bonded phosphate complexes to assess the effect of phosphate ion on the oxidation–reduction photochemistry of other polynuclear metal cores.

Acknowledgment. Support for this research by the National Science Foundation and the Presidential Young Investigator Program is acknowledged. D.G.N. also acknowledges support from the Research Corp., the Amax Foundation, and a Camille and Henry Dreyfus Grant for Newly Appointed Young Faculty in Chemistry. We thank Robert D. Mussell and Mark D. Newsham for their assitance in electrochemical and EPR measurements, respectively. It is a pleasure to acknowledge helpful discussions with Dr. Jay R. Winkler.

(41) Anbar, M. *Adv. Chem. Ser.* **1965**, *No. 50*, 55–81.

(42) Solutions of $IrCl_6^{3-}$ irradiated under N_2O yield $IrCl_6^{2-}$ and N_2. Spectroscopic and photochemical studies support a mechanism in which hydrogen atoms are generated as the primary photoproducts.[43] These results imply that photochemically generated hydrogen atoms react with N_2O to produce N_2.

(43) Eidem, P. K.; Maverick, A. W.; Gray, H. B. *Inorg. Chim. Acta.* **1981**, *50*, 59–64.

(44) Trogler, W. C.; Erwin, D. K.; Geoffroy, G. L.; Gray, H. B. *J. Am. Chem. Soc.* **1978**, *100*, 1160–1163.

(45) Schmidt, W.; Taube, H. *Inorg. Chem.* **1963**, *2*, 698–705.

(46) Ilan, Y. *Inorg. Chem.* **1985**, *24*, 4223–4226.

(47) pH dependence studies of the reported electrochemistry and photochemistry are precluded by the insolubility of the Mo_2 phosphate dimers in H_3PO_4 solutions with concentrations <2 M. We have recently prepared alkyl and aryl Mo_2 phosphates which will allow us to address the effect of pH on these dimers' photochemical and electrochemical properties.